XIV International Conference on Topics in Astroparticle and Underground Physics (TAUP 2015) IOP Publishing
Journal of Physics: Conference Series **718** (2016) 042007 doi:10.1088/1742-6596/718/4/042007

Predictions of hydrodynamic simulations for direct dark matter detection

Nassim Bozorgnia[1,⋆], Francesca Calore[1], Matthieu Schaller[2], Mark Lovell[1,3], Gianfranco Bertone[1], Carlos S. Frenk[2], Robert A. Crain[4], Julio F. Navarro[5,6], Joop Schaye[7] and Tom Theuns[2]

[1] GRAPPA, University of Amsterdam, Science Park 904, 1090 GL Amsterdam, Netherlands
[2] Institute for Computational Cosmology, Durham University, South Road, Durham DH1 3LE, UK
[3] Instituut-Lorentz for Theoretical Physics, Niels Bohrweg 2, NL-2333 CA Leiden, Netherlands
[4] Astrophysics Research Institute, Liverpool John Moores University, 146 Brownlow Hill, Liverpool L3 5RF, UK
[5] Department of Physics & Astronomy, University of Victoria, Victoria, BC, V8P 5C2, Canada
[6] Senior CIfAR Fellow
[7] Leiden Observatory, Leiden University, PO Box 9513, NL-2300 RA Leiden, Netherlands
⋆ presenting author

E-mail: n.bozorgnia@uva.nl

Abstract. We study the effects of galaxy formation on dark matter direct detection using hydrodynamic simulations obtained from the "Evolution and Assembly of GaLaxies and their Environments" (EAGLE) and APOSTLE projects. We extract the local dark matter density and velocity distribution of the simulated Milky Way analogues, and use them directly to perform an analysis of current direct detection data. The local dark matter density of the Milky Way-like galaxies is 0.41– 0.73 GeV/cm^3, and a Maxwellian distribution (with best fit peak speed of 223 – 289 km/s) describes well the local dark matter speed distribution. We find that the consistency between the result of different direct detection experiments cannot be improved by using the dark matter distribution of the simulated haloes.

1. Introduction

Direct dark matter (DM) detection experiments search for the energy deposited by a recoiling nucleus due to the scattering of a DM particle in an underground detector. Currently hints for a DM signal from the DAMA/LIBRA [1] (DAMA for short) and the Si detectors in CDMS-II [2] (CDMS-Si for short) experiments are in strong tension with null results from other experiments. In the analysis of data from direct detection experiments, usually the Standard Halo Model (SHM) is assumed which is an isothermal sphere with isotropic Maxwellian DM velocity distribution. The fiducial value for the local DM density is taken to be 0.3 GeV/cm^3, and the local circular speed at the position of the Sun is assumed to be 220 or 230 km/s.

In this work, which is based on [3], we study the properties of the DM halo as inferred from the high resolution EAGLE [4, 5] and APOSTLE [6, 7] hydrodynamic simulations of galaxy formation, and particularly their implications for DM direct detection. These simulations have been especially calibrated to reproduce the observed stellar mass functions of low redshift galaxies. In particular, we use the EAGLE high resolution (HR) and the APOSTLE intermediate resolution (IR)

simulations, which are comparable in resolution. In addition to the hydrodynamic simulations used in this work, we also present results for dark matter only (DMO) companion simulations in EAGLE and APOSTLE which were run assuming all the matter content is collisionless.

2. Identifying Milky Way analogues

To identify simulated galaxies which are Milky Way (MW) analogues, we first select all haloes with virial mass in the range $(0.5-14)\times10^{12}$ $M_\odot$. We then apply two additional selection criteria which are relevant for predicting the local DM density and velocity distribution accurately: (i) the rotation curve of each simulated halo gives a good fit to the observed MW rotation curve from Ref. [8], and (ii) the stellar mass of the simulated haloes is within the 3σ range of the observed MW stellar mass, $4.5 \times 10^{10} < M_*/M_\odot < 8.3 \times 10^{10}$ [9]. Both criteria are relevant in studying the implications of simulations for dark matter direct detection, since they constrain the local circular speed, v_c, at the Sun's position. The set of simulated galaxies which satisfies our selection criteria consist of 12 galaxies in the EAGLE HR and 2 galaxies in the APOSTLE IR simulations.

3. Local dark matter distribution

Two important parameters which enter in the event rates in DM direct detection experiments are the DM density and velocity distribution at the Solar position. To extract the local DM density and velocity distribution of the selected MW analogues, we consider all particles in a torus aligned with the stellar disc, with $7 < R < 9$ kpc, where R is the galactocentric distance, and a height of $|z| < 1$ kpc with respect to the galactic plane. There are 1821 – 3201 particles in the torus depending on the simulated MW-like galaxy. We find that the average DM density in the torus is in the range of 0.41 – 0.73 GeV/cm^3 for the 14 MW analogues, in agreement with global and local determinations of the local DM density.

The left panel of Fig. 1 shows the local DM speed distribution in the Galactic rest frame for two MW-like haloes which have speed distributions closest to and farthest from the SHM Maxwellian (with peak speed of 230 km/s). The right panel of the same figure shows the speed distributions for the DMO counterparts of the haloes considered in the left panel. The speed distributions are normalized such that $\int dv f(|\mathbf{v}|) = 1$. The range of the best fit local circular speed for the Maxwellian distribution is 223 – 289 km/s in the hydrodynamic case. When baryons are included in the simulation, the galactic gravitational potential deepens in the inner regions of the galaxy, causing a shift in the peak of the DM speed distribution to higher speeds, as can be seen from a comparison of the two panels of Fig. 1.

4. Implications for direct detection

For the case of spin-independent elastic scattering of a DM matter particle χ off a nucleus with mass number A, the differential recoil event rate is given by,

$$\frac{dR}{dE_R} = \frac{\rho_\chi A^2 \sigma_{\rm SI}}{2 m_\chi \mu_{\chi p}^2} F^2(E_R)\, \eta(v_{\rm min}, t), \tag{1}$$

where E_R is the recoil energy, m_χ is the DM mass, ρ_χ is the local DM density, μ_χ is the DM-nucleon reduced mass, $\sigma_{\rm SI}$ is the spin-independent DM-nucleon scattering cross section, and $F(E_R)$ is the form factor. The minimum speed needed for a DM particle to deposit a recoil energy E_R in the detector is $v_{\rm min} = \sqrt{m_A E_R/(2\mu_{\chi A}^2)}$, where m_A is the nucleus mass, and $\mu_{\chi A}$ is the reduced mass of the DM and nucleus. The halo integral which encodes the astrophysics dependence of the recoil rate is given by,

$$\eta(v_{\rm min}, t) \equiv \int_{v>v_{\rm mim}} d^3v \frac{f_{\rm det}(\mathbf{v}, t)}{v}\,, \tag{2}$$

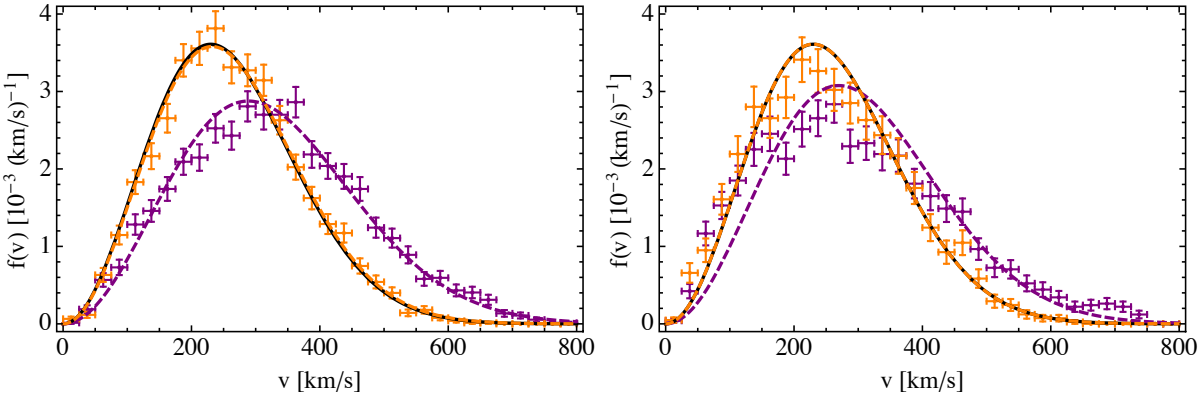

Figure 1. Left: DM speed distributions in the Galactic rest frame for two MW-like haloes with speed distributions closest to (orange data points) and farthest from (purple data points) the SHM Maxwellian (solid black line). The vertical and horizontal error bars specify the 1σ Poisson error on each data point, and the speed bin size (25 km/s), respectively. The dashed lines show the best fit Maxwellian speed distribution for each halo with matching colours. Right: same as left panel but for haloes in a DMO simulation.

where $f_{\rm det}(\mathbf{v}, t)$ is the DM velocity distribution in the detector rest frame. Notice that the velocity of the Earth with respect to the Sun is responsible for the time dependence of the halo integral.

Figure 2 shows the time averaged halo integrals for two MW-like haloes which have speed distributions closest to and farthest from the SHM Maxwellian in the hydrodynamic simulations (left panel) and their DMO counterparts (right panel). The halo integrals for the SHM Maxwellian and the best fit Maxwellians for each halo are shown as solid black line and dashed coloured lines (with matching colours for each halo), respectively. In the hydrodynamic case, the halo integrals obtained from the best fit Maxwellian speed distributions fall within the 1σ uncertainty band of the halo integrals of the simulated haloes. In the DMO simulations, however, this is not the case, and the best fit Maxwellian halo integrals deviate substantially from the halo integrals of the simulated haloes.

We directly use the DM density and velocity distribution of the MW analogues to perform an analysis of data from direct detection experiments, and study how the preferred regions and exclusion limits set by different experiments vary in the DM mass and scattering cross section plane. We consider the positive hints for a DM signal from DAMA [1] and CDMS-Si [2] experiments, and null results from LUX [10] and SuperCDMS [11] experiments.

The left panel of Fig. 3 shows the exclusion limits and allowed regions for the four direct detection experiments obtained for the simulated MW-like haloes with the smallest and largest local DM density. The right panel shows the results for two MW-like haloes with speed distribution closest to and farthest from the SHM Maxwellian. For each halo, the shaded band in the exclusion limits set by LUX and SuperCDMS are obtained from the 1σ uncertainty band of the halo integral. The two allowed regions of the same colour for CDMS-Si, as well as DAMA are also obtained from the upper and lower 1σ limits of the halo integral. The exclusion limits and allowed regions shown in black are obtained assuming the SHM Maxwellian velocity distribution (with peak speed of 230 km/s) and a local DM density of 0.3 GeV/cm^3.

It is clear from Fig. 3 that the main shift in the exclusion limits and preferred regions compared to the SHM is due to the different local DM density of the simulated MW analogous. The effect of the velocity distribution is only at low DM masses, where the experiments are

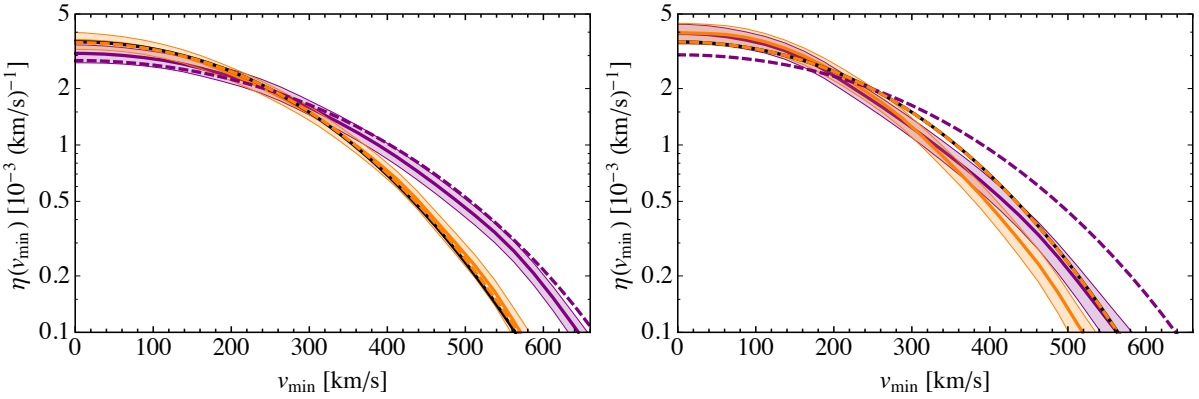

Figure 2. Left: Time averaged halo integrals as a function of $v_{\rm min}$ obtained from the mean velocity distribution (solid coloured lines) and the velocity distribution at $\pm 1\sigma$ from the mean (shaded bands) for the two MW analogues closest to (orange) and farthest from (magenta) the SHM Maxwellian (black line). The halo integral obtained from the best fit Maxwellian speed distribution for each halo is shown by dashed coloured lines with matching colours. Right: Halo integrals for the DMO counterparts of the haloes shown in the left panel.

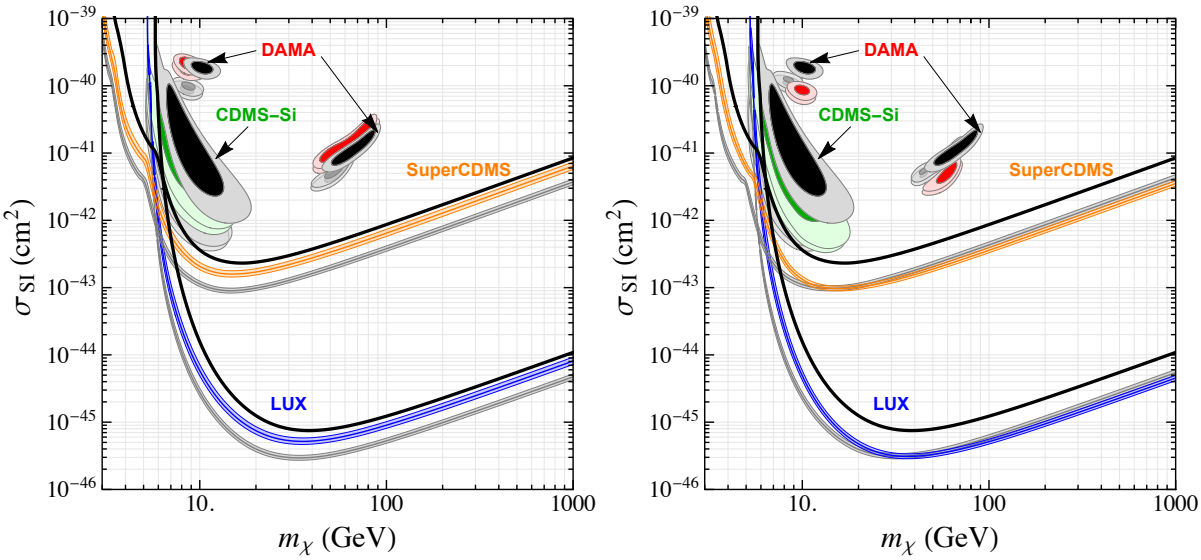

Figure 3. Allowed regions from DAMA (at 90% CL and 3σ) and CDMS-Si (at 68% and 90% CL) and exclusion limits from LUX and SuperCDMS (at 90% CL) in the $m_\chi - \sigma_{\rm SI}$ plane for two MW-like haloes with smallest (shown in colour) and largest (shown in gray) local DM density (left panel), and two haloes with speed distributions closest to (shown in colour) and farthest from (shown in gray) the SHM Maxwellian (right panel). For each halo, the shaded exclusion band and the two adjacent allowed regions of the same colour are obtained from the upper and lower 1σ limits of the halo integral. The black exclusion limits and allowed regions assume the SHM Maxwellian.

sensitive to the high velocity tail of the speed distribution.

5. Summary

In this work, we have studied the implications of the EAGLE and APOSTLE hydrodynamic simulations for DM direct detection. We identified a set of 14 simulated haloes which satisfy observational constraints on the MW. The local DM density for the MW analogues which satisfy our selection criteria is in the range of 0.41 – 0.73 GeV/cm^3. The range of the best fit peak speed of the Maxwellian distribution is 223 – 289 km/s for the simulated haloes in the hydrodynamic simulations, and the halo integrals obtained from the best fit Maxwellian distributions fall within the 1σ uncertainty band of the halo integral of the simulated haloes.

The largest shift in the exclusion limits and allowed regions in the m_χ–$\sigma_{\rm SI}$ plane set by different direct detection experiments for the simulated haloes compared to the SHM is due to the different local DM density of the simulated haloes compared to the fiducial value of 0.3 GeV/cm^3 in the SHM. The effect of the different velocity distribution of the simulated haloes compared to the SHM Maxwellian is only prominent at lower DM masses, where the experiments probe larger $v_{\rm min}$. Notice that for each halo, the allowed regions and exclusion limits set by different experiments shift in the same direction, and hence the consistency between the results of different experiments cannot be improved.

Acknowledgments

N.B. acknowledges support from the European Research Council through the ERC starting grant WIMPs Kairos. This work was supported by the Science and Technology Facilities Council (grant number ST/F001166/1); Interuniversity Attraction Poles Programme initiated by the Belgian Science Policy Office (AP P7/08 CHARM). This work used the DiRAC Data Centric system at Durham University, operated by the Institute for Computational Cosmology on behalf of the STFC DiRAC HPC Facility (www.dirac.ac.uk). This equipment was funded by BIS National E-infrastructure capital grant ST/K00042X/1, STFC capital grant ST/H008519/1, and STFC DiRAC Operations grant ST/K003267/1 and Durham University. DiRAC is part of the National E-Infrastructure. We acknowledge PRACE for awarding us access to the Curie machine based in France at TGCC, CEA, Bruyères-le-Châtel.

References

[1] Bernabei R, Belli P, Cappella F, Caracciolo V, Castellano S *et al.* 2013 *Eur.Phys.J.* **C73** 2648 (*Preprint* 1308.5109)
[2] Agnese R *et al.* (CDMS Collaboration) 2013 *Phys.Rev.Lett.* **111** 251301 (*Preprint* 1304.4279)
[3] Bozorgnia N, Calore F, Schaller M, Lovell M, Bertone G, Frenk C S, Crain R A, Navarro J F, Schaye J and Theuns T 2016 *In preparation*
[4] Schaye J, Crain R A, Bower R G, Furlong M, Schaller M, Theuns T, Dalla Vecchia C, Frenk C S, McCarthy I G, Helly J C, Jenkins A, Rosas-Guevara Y M, White S D M, Baes M, Booth C M, Camps P, Navarro J F, Qu Y, Rahmati A, Sawala T, Thomas P A and Trayford J 2015 *Mon.Not.Roy.Astron.Soc.* **446** 521–554 (*Preprint* 1407.7040)
[5] Crain R A, Schaye J, Bower R G, Furlong M, Schaller M, Theuns T, Dalla Vecchia C, Frenk C S, McCarthy I G, Helly J C, Jenkins A, Rosas-Guevara Y M, White S D M and Trayford J W 2015 *Mon.Not.Roy.Astron.Soc.* **450** 1937–1961 (*Preprint* 1501.01311)
[6] Sawala T, Frenk C S, Fattahi A, Navarro J F, Bower R G, Crain R A, Dalla Vecchia C, Furlong M, Helly J C, Jenkins A, Oman K A, Schaller M, Schaye J, Theuns T, Trayford J and White S D M 2015 *ArXiv e-prints* (*Preprint* 1511.01098)
[7] Fattahi A, Navarro J F, Sawala T, Frenk C S, Oman K A, Crain R A, Furlong M, Schaller M, Schaye J, Theuns T and Jenkins A 2015 *ArXiv e-prints* (*Preprint* 1507.03643)
[8] Iocco F, Pato M and Bertone G 2015 *Nature Phys.* **11** 245?248 (*Preprint* 1502.03821)
[9] McMillan P J 2011 *Mon.Not.Roy.Astron.Soc.* **414** 2446–2457 (*Preprint* 1102.4340)
[10] Akerib D *et al.* (LUX Collaboration) 2014 *Phys.Rev.Lett.* **112** 091303 (*Preprint* 1310.8214)
[11] Agnese R *et al.* (SuperCDMS Collaboration) 2014 *Phys.Rev.Lett.* **112** 241302 (*Preprint* 1402.7137)